Analysis on End-face Temperature of High-speed Oil-Gas Two-Phase Backflow Pumping Seal

IOP Conf. Series: Materials Science and Engineering **544** (2019) 012034 doi:10.1088/1757-899X/544/1/012034

Analysis on End-face Temperature of High-speed Oil-Gas Two-Phase Backflow Pumping Seal

S X Li*, L Chen, H Li, S C Li and Q Z Li

College of Mechanical and Electrical Engineering, Beijing University of Chemical Technology, Beijing, China

E-mail: buctlsx@126.com

Abstract. This paper aims to analyze the end-face temperature in the open state & unopened state, and to verify the feasibility of oil-gas two-phase backflow pumping seal (OG-BPS) in oil-gas two-phase lubrication conditions. The thermal boundary, shear heat, heat distribution, convection heat transfer coefficient and other relevant conditions are applied to the theoretical models establishing. The effect of the seal operation parameters such as the speed, pressure difference and liquid-gas ratio on the end-face temperature is analyzed by calculating the thermo-structural coupling models and conducting experiments. The results show that the end-face temperature in the unopened state is much higher than that in the open state, which can be regarded as a criterion for whether the seal works normally. In the open state, the end-face temperature increases slightly with the increase of the rotation speed and liquid-gas ratio. In the unopened state, the end-face temperature increases sharply with the increase of the rotation speed and the pressure difference. However, with the increases of the liquid-gas ratio, the end-face temperature will decrease rapidly, so the oil-gas two-phase medium will be beneficial to start-stop operation. This paper verifies the feasibility of the OG-BPS, and provides a basis for further study of the effect of end temperature on seal performance.
Key words: oil-gas, end-face temperature, backflow pumping, thermo-structural coupling

1. Introduction

In recent years, as the speed of rotating equipment continues to increase, oil-gas two-phase lubrication technology is widely used in high-speed conditions, because of its high efficiency, good lubrication effect, energy consumption and other advantages [1-3]. However, the sealing problem of oil-gas two-phase lubrication has become a bottleneck restricting its development [4]. Under the oil-gas two-phase condition, the traditional single-medium seal is no longer applicable [5].

Nowadays, a non-contact dynamic pressure seal has been developed for high-speed bearing cavity of aircraft engines under oil-gas two-phase lubrication conditions, such as a high-performance fluid film seal device developed by NASA, which mainly used in aviation high-speed bearing cavity by using hydrodynamic and hydrostatic lubrication principle [6]. Research on single medium seal such as dry gas seal and upstream pumping seal are mainly focused on the influence of dynamic pressure tank groove design & optimization, operating & structure parameters, dynamic state, fluid film thermal behavior and so on [7-9].

However, the theoretical research on end-face temperature in the gas-liquid two-phase mixed medium is relatively less. During the start-stop phase of the seal, the dry friction occurs between the end-faces and the end-face temperature rises sharply, which in turn causes thermal deformation and

thermal stress. At the same time, changes in temperature may result in changes in the phase state of the seal medium, and it can easily lead to seal failure [10]. The end-face temperature not only affects the end-face deformation but also characterizes the friction state of the end-face. Monitoring and analyzing the end-face temperature is conductive to study the mechanism of high temperature failure. Therefore, the theoretical and experimental research on the end-face temperature of the OG-BPS is of great significance.

2. Working principle

Figure 1a &1b is the structure and grooved face of OG-BPS. The outer side of the seal is oil and gas, the inside is the atmosphere. When the rotation speed exceeds a certain range, the oil will be disintegrated into small oil droplets under the combined action of high stirring force of the rotating element and its own centrifugal force, and the oil droplets are fully mixed with air to form the oil-gas two-phase medium.

There are micro scale spiral grooves at low-pressure side of rotary ring. When the seal is working, the fluid at high-pressure side enters the end-face from the outside of the seal ring, part of the fluid leaks to the low-pressure side, due to the existence of the spiral groove, the leaking fluid will be passively sucked into the slot and will rotate along with the groove. When the fluid moves to the root of the spiral groove, the flow path narrows and the fluid accumulates here, producing a high-pressure zone and acting as a sealing effect. At the same time, the fluid is pumped back from the low-pressure side to the high-pressure side, which is the effect of the “backflow pumping”, thereby achieving “zero leakage”.

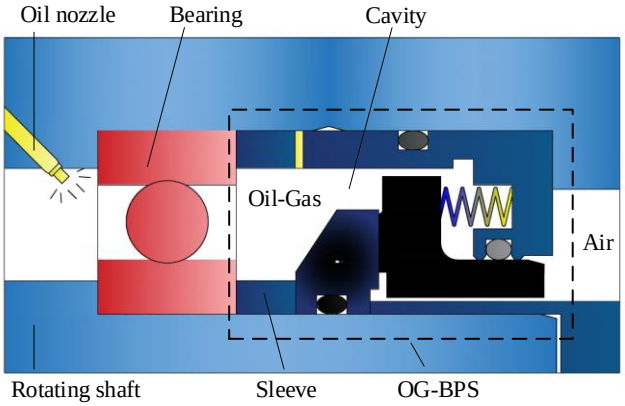

Figure 1a. The structure of OG-BPS.

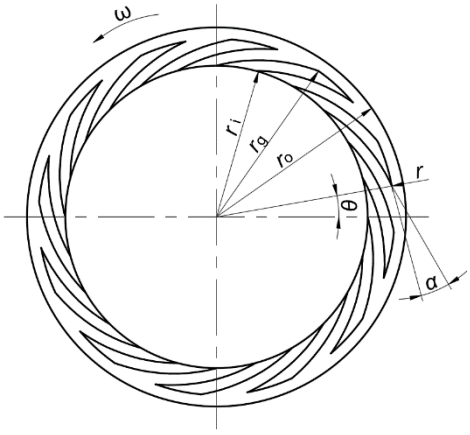

Figure 1b. Grooved face of OG-BPS.

When the rotation speed is lower than the opening speed, the seal rings are in contact with each other, said the state is **unopened state**. When the rotation speed is higher than the opening speed, the seal rings are not in contact with each other, said the state is **open state**. Due to the different heat transfer mechanism of the two states, the following analysis is performed separately.

3. Thermal-solid coupling analysis model

3.1. Physical model

The shape of the groove is a logarithmic spiral, the expression is:

$$r = r_g e^{\theta \tan \alpha} \tag{1}$$

Where r_g is the groove root radius; θ is the rotate-angle; α is the spiral groove angle.

The specific structure size and operating parameters of OG-BPS are shown in Table 1.

Table 1. The structure and operating parameters of OG-BPS.

Parameter	Value
Outside radius r_o/mm	57.5
Groove root radius r_g/mm	55
Inside radius r_i/mm	50
Spiral groove angle α/°	20
Spiral groove depth h_g/μm	5
Land-to-groove ratio γ	0.5
Dam-to-groove ratio δ	0.7
Number of spiral grooves N_g	12
Medium	Air and Mobil jet Oil II
Pressure of oil-gas p_i/MPa	0.15
Pressure of air p_o/MPa	0.05
Operating temperature T/°C	26
Shaft speed n/rpm	8000
Rotary ring material	SiC
Static ring material	C

In view of the centrally symmetric and periodic distribution of the OG-BPS geometric model, a cycle of the seal ring is selected as the calculation area for analysis. The periodic boundary condition is:

$$\begin{cases} \varphi(r,\theta_2,z)=\varphi(r,\theta_1,z) \\ \theta_2=\theta_1+2\pi/N_g \end{cases} \tag{2}$$

The model in the open state is divided into two parts: fluid domains and solid domains.

3.2. Thermal balance analysis

Due to the complicated seal boundaries, the following assumptions are made [11]:

a. Assuming a steady-state temperature field;
b. All the heat is transmitted by the seal rings;
c. Heat flux density on the seal ring end-faces is evenly distributed;
d. The place where the seal elements contact the seal rings is convection heat transfer;
e. The boundary where contacts the O-ring is the adiabatic boundary;
f. The nature of medium and seal rings does not change with temperature.

Figure 2a &2b is the theoretical model of seal rings. In the open state, the viscous shear heat is QV. In the unopened state, the friction heat is QF.O-ring friction heat and the spring vibration heat is QG, which is small and can be neglected. Heat dissipation includes QA1, QA2 (convection heat transfer of surface and oil-gas), QB1, QB2 (convection of static ring and oil-gas, air), QC1, QC2 (the heat rotary ring delivered to the shaft, static ring delivered to the static seat), QD1, QD2 (the heat of the fluid flowing out of the seal end-faces). According to the calculation results of the micro-flow field, the mass flow of the medium at the inlet and outlet is very small, which is on the order of 10-6g·s-1, so it can be regarded as zero leakage [12].

The theoretical thermal equilibrium condition is:

$$Q_V(Q_F)+Q_G=Q_{A1}+Q_{A2}+Q_{B1}+Q_{B2}+Q_{C1}+Q_{C2}+Q_{D1}+Q_{D2}$$

After simplified:

$$Q_V(Q_F) = Q_{A1} + Q_{A2} + Q_{B1} + Q_{B2} + Q_{C1} + Q_{C2}$$

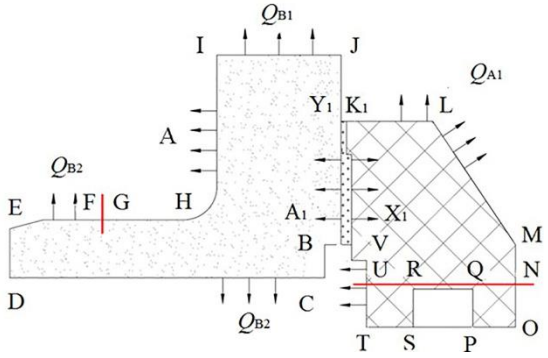

Figure 2a. Theoretical model in open state.

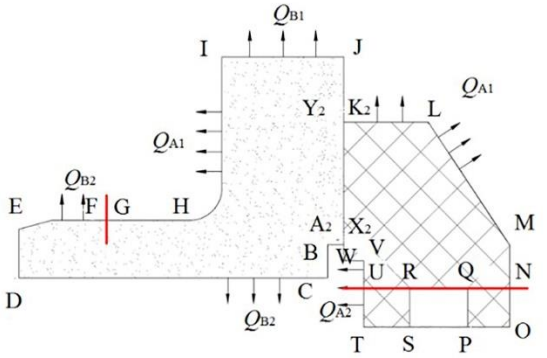

Figure 2b. Theoretical model in unopened state.

3.3. Boundary conditions

According to the structure, the thermal boundary conditions [13] is in Table 2.

Table 2. Thermal boundary of OG-BPS

Thermal boundary conditions	Boundary name
Viscous shear heat generation of end-faces and two-phase fluid	Y_1A_1、K_1X_1
Friction heat between end-faces	Y_2A_2、K_2X_2
Convection heat transfer between rotary ring and medium	KL、LM、MN、NO
Convection heat transfer between rotary ring and air	TS、TU、UV、VW、WX
Static ring and oil-gas two-phase medium	YJ、JI、IH、HG
Convection heat transfer between static ring and air	EF、ED、DC、CB、AB
Contact with the O-ring is considered adiabatic	SR、RQ、QP、FG

The force boundary conditions in the unopened state is in Table 3.

Table 3. Force boundary conditions setting

Force boundary conditions	Boundary name
Oil and gas two-phase medium pressure	GH、HI、IJ、JY、KL、LM、MN、PO、PQ、RQ
Atmospheric pressure	GF、FE、ED、DC、CB、BA、XW、WV、VU、TS
Spring pressure	HI
O-ring pressure	RS
Mixed fluid membrane back pressure	Y_2A_2、K_2X_2
Full constraint	ED、JK
Contact constraint	VM、WL

3.4. Viscous shear heat (Q_V) calculation

The viscous shear heat can be obtained as follows [14]:

$$Q_{\mathrm{V}} = q_{\mathrm{V}} \times A_{\mathrm{f}} \tag{3}$$

Where q_{v} is the heat flux density; A_{f} is the area of the seal end-face.

3.5. Heat distribution of the seal rings

The heat distribution on the two seal rings is different, and the thermal steady-state temperature can be obtained as follows [15]:

$$T = q_{\mathrm{V}}(h_1 - y) / \lambda \tag{4}$$

Where h_1 is the axial thickness of the seal ring; y is the distance from the end-face; λ is the thermal conductivity of the seal ring.

The temperature of the two rings at the end-face is equal, so when $y = 0$, there is:

$$\begin{cases} q_{\mathrm{r}} h_{\mathrm{r}} / \lambda_r = q_{\mathrm{s}} h_{\mathrm{s}} / \lambda_{\mathrm{s}} \\ q_{\mathrm{w}} + q_{\mathrm{s}} = q \end{cases} \tag{5}$$

The heat flux density of the rotary ring & static ring can be obtained as follows:

$$\begin{cases} q_{\mathrm{s}} = q / (1 + h_{\mathrm{s}} \lambda_{\mathrm{w}} / h_{\mathrm{w}} \lambda_{\mathrm{s}}) \\ q_{\mathrm{w}} = q - q_{\mathrm{s}} \end{cases}$$

The heat flux density in unopened state can be obtained as follows [16]:

$$q_{(i)} = 2\pi n r_{(i)} f p_{(i)} \tag{6}$$

Where $q_{(i)}$ is the heat flux density of point i; $p_{(i)}$ is the contact pressure of point i; n is the rotating speed; $r_{(i)}$ is the radius of point i.

3.6. Convection heat transfer coefficient [16]

The convection heat transfer coefficient of rotary ring and oil-gas can be obtained in equation (7). The convection heat transfer coefficient of rotary ring and air can be obtained in equation (8). There is no swirling flow in the flow around the static ring and its surroundings, so the convective heat transfer coefficient is given by equation (9).

$$\alpha_1 = \frac{\lambda}{d_{\mathrm{o}}} \cdot 0.135 \cdot \left[\left(0.5 Re_{\mathrm{e}}^2 + Re_{\mathrm{f}}^2 \right) \cdot Pr \right]^{0.33} \tag{7}$$

$$\alpha_2 = \frac{0.21\lambda}{2S_{\mathrm{s}}} \cdot \left(Ta^2 \cdot Pr \right)^{0.25} \tag{8}$$

$$\alpha_3 = \frac{0.023\lambda}{2S_{\mathrm{s}}} \cdot \left(\varepsilon_1 \cdot Re^{0.8} Pr^{0.4} \right) \tag{9}$$

4. Temperature field calculation and analysis

4.1. Temperature field cloud char

The temperature field cloud chart in open state is shown in Figure 3a &3b. The temperature of rotary ring is lower than that of static ring because the former is at oil-gas side and rotates at high speed, so the convective heat transfer of rotary ring is stronger than that of static ring.

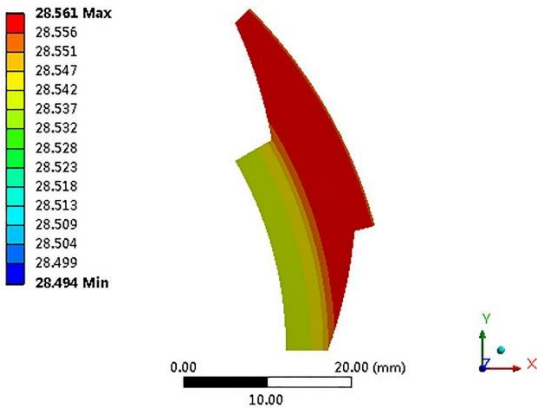

Figure 3a. Rotary ring temperature field.

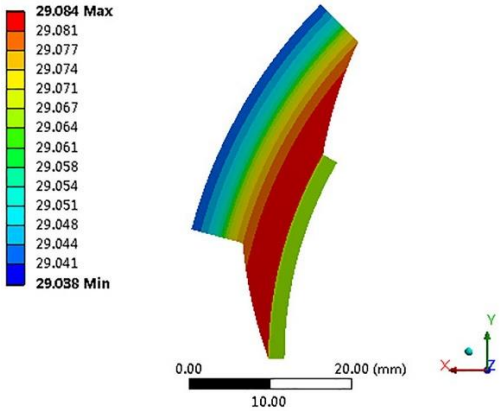

Figure 3b. Static ring temperature field.

The temperature field cloud chart in unopened state is shown in Figure 4a &4b. The heat flux density will be larger with the contact pressure or speed increases; therefore, the highest temperature point is at the outside radius side where the seal rings contact. The static ring (graphite ring) has a larger thermal conductivity, so its temperature gradient is greater than that of the rotary ring.

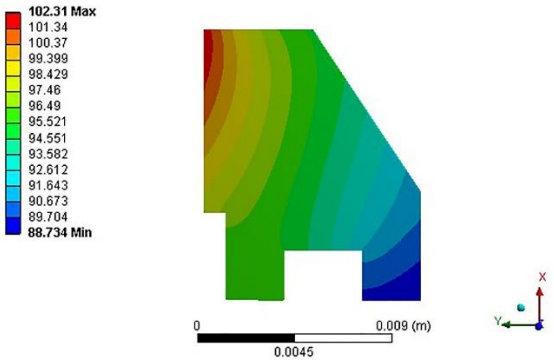

Figure 4a. Rotary ring temperature field.

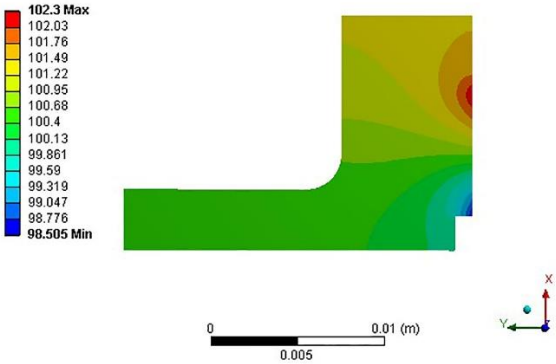

Figure 4b. Static ring temperature field.

4.2. Effect of operating parameters on the end-face temperature field

4.2.1. Rotation speed. In Figure 5, with the increase of rotation speed, both the viscous shear heat and frictional heat increases, so the temperature rise of the end-face increases. At the same time, the rotation speed makes the convection heat transfer coefficient increase, which enhances the heat transfer, so the end-face tempera¬ture increases slowly.

4.2.2. Pressure difference. In Figure 6, the frictional heat in the unopened state increases with the pressure difference increases, while the convection heat transfer coefficient on the seal ring remains constant. Therefore, as the pressure difference increases, the end-face temperature increases linearly.

4.2.3. Liquid-gas ratio. In Figure 7, in the unopened state, when the liquid-gas ratio increases, the convective heat transfer effect is enhanced and the temperature drops significantly. In the open state, due to the combined effect of shear heat and convection heat transfer, the liquid-gas ratio has little effect on the temperature change.

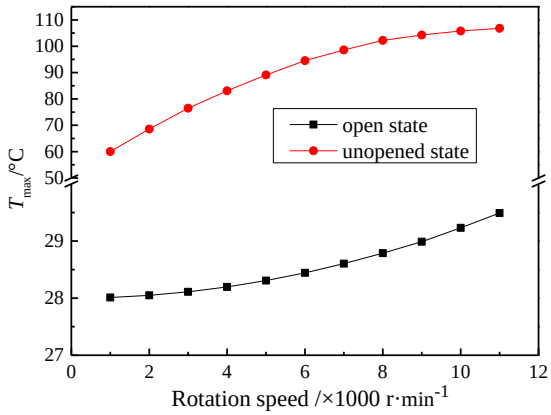

Figure 5. The effect of rotation speed on temperature.

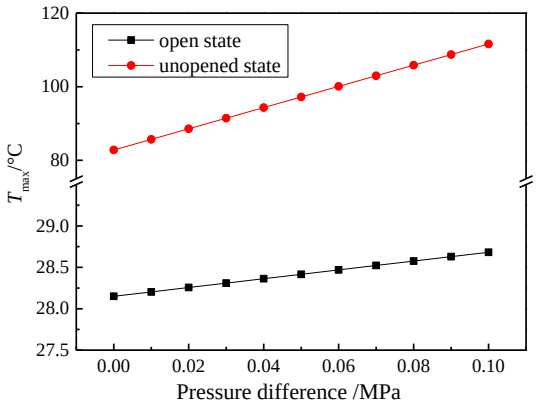

Figure 6. The effect of pressure difference on temperature.

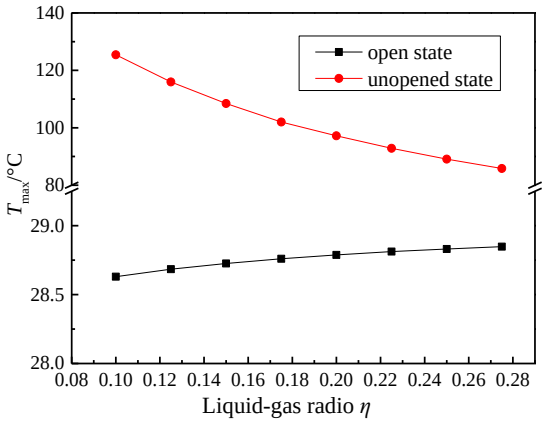

Figure 7. The effect of liquid-gas ratio on temperature.

5. Experimental verification

The variable speed, variable pressure and variable lubrication conditions tests have been carried out to verify the correctness of the numerical results.

5.1. Experimental equipment

The experiment equipment of OG-BPS is shown in Figure 8a &8b.

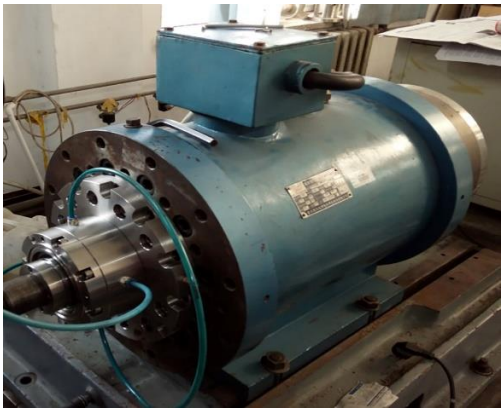

Figure 8a. Experiment bench.

Figure 8b. The innstallation of thermocouple.

5.2. The effect of rotation speed on the end-face temperature

As shown in Figure 9, the sealing end face is opened at about 3000 rpm. The rotational speed has a greater influence on the end face temperature in the unopened state, and has less influence on the end face temperature in the open state. When the speed increases to a certain value, the end face is opened and the seal ring will have a slight temperature rise due to the dry friction before opening. The test results are basically consistent with the calculation results.

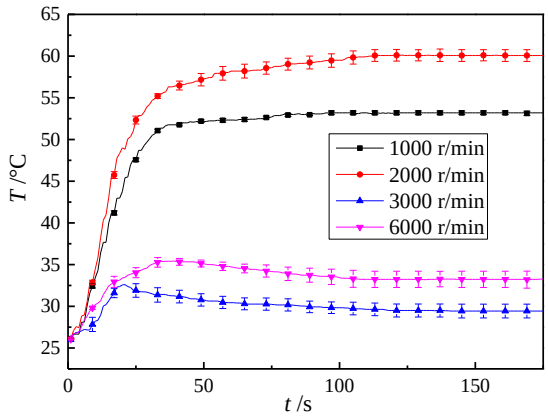

Figure 9. Temperature change curve under different rotation speed.

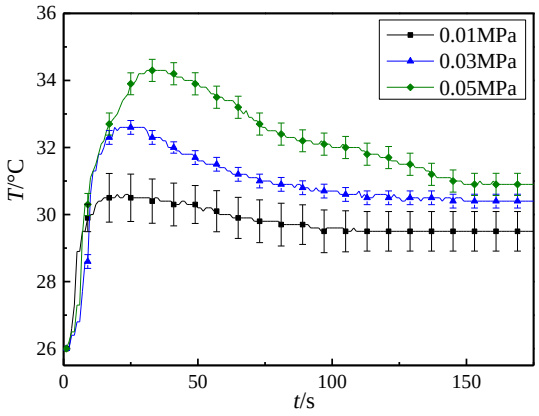

Figure 10. Temperature change curve under different pressure.

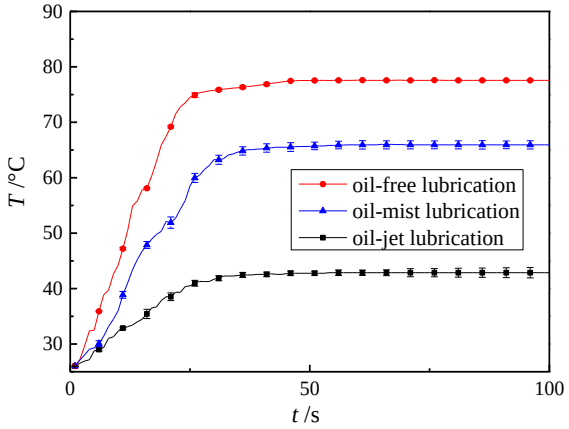

Figure 11. Temperature curve under different lubrication condition in the unopened state.

5.3. The effect of different pressure on end-face temperature

As shown in Figure 10, the differential pressure has a significant effect on the end face temperature only in the unopened state. When the seal is in the open state, the viscous shear heat of the fluid is the only source of heat, the value of which is much lower than the heat of solid friction, so the temperature rise is small. The test results are basically consistent with the numerical calculation results.

5.4. The effect of different oil-gas radio on end-face temperature

As shown in Figure 11, the test result is slightly higher than the numerical calculation result, because the seal is in the open state in the test, and the temperature rise mainly comes from the friction heat in the unopened state. When the seal is in an oil-free lubrication state, the temperature rise is the largest, followed by the oil mist lubrication, and the injection lubrication is minimal. Therefore, the lubricating oil has a great cooling effect on the seal.

6. Conclusion

The end-face temperature in the open state is much lower than that in the unopened state, so it can be used as a criterion for whether the seal end-face is open. The speed should be quickly increased/decreased in the start/stop phase, in order to avoid prolonged stay at low speed stage and prevent the seal rings thermal cracking damage. Oil-gas lubrication is conducive to the start/stop phase. Seal ring with different structural parameters has different convection heat transfer coefficients, therefore, the effect of temperature on the seal performance can be reduced by optimizing the structure of seal ring. In working condition, with the change of these three variables (rotation speed, pressure and liquid-gas ratio), the amplitude of the change is relatively small and the temperature is relatively low, OG-BPS can work stably and reliably under changing conditions. The experiment results are in agreement with the numerical results, which proves the correctness of the numerical calculation.

References

[1] Kim K T 1997 The Effect of Oil-Starvation on the Lubrication Characteristics of High-Speed Bearing: Part II-Roller Bearing *Journal of Clinical Microbiology* **34** 447-9
[2] Liu H B, Wang H Y, Lei Z, Shi Y S and Liu G P 2016 Analysis on penetration mechanism of oil jet lubrication for high speed rolling bearing *Journal of Aerospace Power*
[3] Rucker G, Weidmann W and Reisenweber K U 1983 Rotary ring seal with gas-dynamic lubrication for high-speed turbomachines. US)
[4] Xue yong L I and Fang G H 2016 Analysis on Oil-air Lubrication for Guide of Finish Rolling for High Speed Wire Rod Plant of Baotou Steel and Improvement of Oil Way *Science & Technology of Baotou Steel*
[5] Li X F, Cai J N, Zhang Q X and Li S X 2016 Analysis on Hydrodynamic Sealing Performance under Low Liquid-gas Ratio Mixed Lubrication *Lubrication Engineering* **41** 40-44
[6] Hu G Y 2012 Application Research of Seal Technologies for Aeroengine *Aeroengine* **38** 1-4
[7] Hu S T, Huang W F, Liu X F and Wang Y M 2017 Applicability Analysis of Steady-state Models for Spiral Groove Gas Face Seals *Journal of Mechanical Engineering* **53** 7-13
[8] Wang Q, Chen H L, Liu T, Liu Y H, Liu Z B and Liu D H 2012 Research on performance of upstream pumping mechanical seal with different deep spiral groove. p 2019
[9] Xu H J, Song P Y and Yu J P 2013 Analysis on the Seal Performance of Aerostatic Gas Lubricating Mechanical Seal Lubrication Engineering 41-45
[10] Zhang G, Zhao W and Tian Y X 2014 Experimental study on the water lubrication of non-contacting face seals for turbopumps *Industrial Lubrication & Tribology* **66** 314-21
[11] Ding X X, Wu H, Yan R Q, Liu Y and Yan F 2014 Analysis and calculation of thermal stressing coupled deformation of mechanical seal based on ANSYS *Journal of Lanzhou University of Technology* **40** 41-45
[12] Wang Y T 2015 The Analysis of Mechanical Seal's Leakage Rate *Hydraulics Pneumatics & Seals* **35** 40-42
[13] Zhang Z S, Yang Y M, Dai X D and Xie Y B 2014 Effects of Thermal Boundary Conditions on Thermo¬hydrodynamic Lubrication Analysis of Plain Journal Bearing *China Mechanical Engineering* **25** 1427-1432
[14] Cheng W Q 2013 Numerical Simulation of Scramjet Combustor Based on the Orthogonal Experimental Design. Nanchang Hangkong University
[15] Li N, Zhu W B, Wang H S and Wang Y F 2009 Research on Distribution Law of Steady-state Temperature for the Rotating Ring of T-shape Groove Dry Gas Seal *Chinese Hydraulics & Pneumatics* 46-49
[16] Wang Z T, Zhang Q X, Cai J N Huang B C and Li S X 2015 Analysis on Thermal Characteristic of Hot Oil Pump Mechanical Seal *Lubrication Engineering* **40** 20-25